Journal of Energy

VOLUME 61 Number 1–4 | 2012 Special Issue

journal homepage: http://journalofenergy.com/

Oszkár Bíró
Graz University of Technology
biro@tugraz.at

Gergely Koczka
Graz University of Technology
gergely.koczka@tugraz.at

Bernhard Wagner
Siemens Transformers Austria
bernhard.a.wagner@siemens.com

Ulrike Baumgartner
Siemens Transformers Austria
ulrike.baumgartner@siemens.com

Gerald Leber
Siemens Transformers Austria
gerald.leber@siemens.com

FINITE ELEMENT METHOD FOR NONLINEAR EDDY CURRENT PROBLEMS IN POWER TRANSFORMERS

SUMMARY

An efficient finite element method to take account of the nonlinearity of the magnetic materials when analyzing three dimensional eddy current problems is presented in this paper. The problem is formulated in terms of vector and scalar potentials approximated by edge and node based finite element basis functions. The application of Galerkin techniques leads to a large, nonlinear system of ordinary differential equations in the time domain.

The excitations are assumed to be time-periodic and the steady state periodic solution is of interest only. This is represented in the frequency domain as a Fourier series for each finite element degree of freedom and a finite number of harmonics is to be determined, i.e. a harmonic balance method is applied. Due to the nonlinearity, all harmonics are coupled to each other, so the size of the equation system is the number of harmonics times the number of degrees of freedom.

The harmonics would be decoupled if the problem were linear, therefore, a special nonlinear iteration technique, the fixed-point method is used to linearize the equations by selecting a time-independent permeability distribution, the so called fixed-point permeability in each nonlinear iteration step. This leads to uncoupled harmonics within these steps resulting in two advantages. One is that each harmonic is obtained by solving a system of algebraic equations with only as many unknowns as there are finite element degrees of freedom. A second benefit is that these systems are independent of each other and can be solved in parallel. The appropriate selection of the fixed point permeability accelerates the convergence of the nonlinear iteration.

The method is applied to the analysis of a large power transformer. The solution of the electromagnetic field allows the computation of various losses like eddy current losses in the massive conducting parts (tank, clamping plates, tie bars, etc.) as well as the specific losses in the laminated parts (core, tank shielding, etc.). The effect of the presence of higher harmonics on these losses is investigated.

Key words: Finite element method, fixed point technique, harmonic balance method, nonlinearity, parallel computation

O. Bíró, U. Baumgartner, G. Koczka, G. Leber, B. Wagner, Finite element method for nonlinear eddy current problems in power transformers, Journal of Energy, vol. 61 Number 1–4 (2012) Special Issue, p. 87-96

https://doi.org/10.37798/2012611-4240

1. INTRODUCTION

The saturation of iron parts of transformers gives rise to the presence of higher harmonics in the electromagnetic fields, leading to additional losses. The prediction of these losses is important in the design of large power transformers. A method for the analysis of transformer losses has been presented in [1] with the assumption of sinusoidal time variation, i.e. neglecting higher harmonics. The present paper extends this method for the case of general periodic time variation.

The most straightforward method of solving nonlinear electromagnetic field problems in the time domain by the method of finite elements (FEM) is using time-stepping techniques. This requires the solution of a large nonlinear equation system at each time step and is, therefore, very time consuming, especially if a three-dimensional problem is being treated. If the excitations are non-periodic or if, in case of periodic excitations, the transient solution is required, one cannot avoid time-stepping. In many cases however, the excitations of the problem are periodic, and it is only the steady-state periodic solution which is needed. Then, it is wasteful to step through several periods to achieve this by the "brute force" method [2] of time stepping.

A time domain technique using the fixed-point method to decouple the time steps has been introduced in [3] and applied to two-dimensional eddy current problems described by a single component vector potential. The optimal choice of the fixed point permeability for such problems has been presented in [4] both in the time domain and using harmonic balance principles. The method has been applied to three-dimensional problems in terms of a magnetic vector potential and an electric scalar potential (**A**,*v*-**A** formulation) in [5] and, employing a current vector potential and a magnetic scalar potential (**T**,Φ-Φ formulation), in [6] and [7].

The aim of this work is to show the application of the method to industrial problems arising in the design of large power transformers. In this context, the computation of losses due to higher saturation harmonics is investigated.

The paper is structured as follows: In the following two sub-sections of the Introduction, two FEM potential formulations of eddy current problems are briefly reviewed and the harmonic balance method to obtain their steady state periodic solution is introduced. In section 2, a method is developed to decouple the harmonics from each other and hence to solve for each harmonic separately. This is trivial for linear problems, but a special fixed point iteration technique is introduced to treat nonlinearity with the harmonics decoupled. Section 3 is devoted to a numerical example involving a large power transformer. The losses due to higher harmonics are computed and analyzed here. The results of the paper are concluded in section 4.

1.1. Finite element potential formulations

The electromagnetic field problem to be solved in the eddy current domain Ω_c (such as the tank, the clamping plates and tie bars as well as some laminates at the core boundary exposed to stray fields) is described by Maxwell's equations in the quasi-static limit:

$$curl\mathbf{H} = \mathbf{J} + curl\mathbf{T}_0\,, \tag{1}$$

$$curl\mathbf{E} = -\frac{\partial \mathbf{B}}{\partial t}\,, \tag{2}$$

$$div\mathbf{B} = 0\,, \tag{3}$$

$$div\mathbf{J} = 0 \tag{4}$$

where: **H** is the magnetic field intensity, **J** is the eddy current density, $\mathbf{T}_0$ is a current vector potential whose curl is the given current density in the windings, **E** is the electric field intensity, **B** is the flux density and *t* is time. In the insulating region Ω_n (such as oil and air domains, the windings, as well as laminated parts free of eddy currents) it is sufficient to solve (1) with **J=0** in addition to (3) for the magnetic field quantities. The material relationships are

$$\mathbf{B} = \mu\left(|\mathbf{H}|\right)\mathbf{H} \text{ or } \mathbf{H} = \nu\left(|\mathbf{B}|\right)\mathbf{B} \tag{5}$$

$$\mathbf{J} = \sigma\mathbf{E} \text{ or } \mathbf{E} = \rho\mathbf{J} \tag{6}$$

O. Bíró, U. Baumgartner, G. Koczka, G. Leber, B. Wagner, Finite element method for nonlinear eddy current problems in power transformers, Journal of Energy, vol. 61 Number 1–4 (2012) Special Issue, p. 87-96

where: μ is the permeability, ν is its reciprocal, the reluctivity and σ is the conductivity with ρ denoting its reciprocal, the resistivity. In magnetic materials (steel), the relationships (5) are nonlinear, i.e. the permeability and the reluctivity depend on the magnetic field intensity or the magnetic flux density as indicated.

The numerical solution of the problem is carried out by the method of finite elements. The application of FEM is straightforward if potential functions are introduced. Basically, two options are open: the field quantities can either be represented by a magnetic vector potential **A** and an electric scalar potential *v* (**A**,*v*-**A** formulation) as

$$\mathbf{B} = curl\mathbf{A} \text{ in } \Omega_c \cup \Omega_n,\ \mathbf{E} = -\frac{\partial}{\partial t}\left(\mathbf{A} + gradv\right) \text{ in } \Omega_c, \tag{7}$$

or by a current vector potential **T** and a magnetic scalar potential Φ (**T**,Φ-Φ formulation) as

$$\mathbf{H} = \mathbf{T}_0 + \mathbf{T} - grad\Phi \text{ in } \Omega_c \cup \Omega_n,\ \mathbf{J} = curl\mathbf{T} \text{ in } \Omega_c \tag{8}$$

with **T=0** in Ω_n. The definitions (7) satisfy (2) and (3), whereas those in (8) ensure that (1) and (4) hold. Therefore, the differential equations (1) and (4) are to be solved in the **A**,*v*-**A** formulation:

$$curl\left(\nu curl\mathbf{A}\right) + \frac{\partial}{\partial t}\left[\sigma\left(\mathbf{A} + gradv\right)\right] = curl\mathbf{T}_0, \tag{9}$$

$$-div\left[\sigma\frac{\partial}{\partial t}\left(\mathbf{A} + gradv\right)\right] = 0, \tag{10}$$

and the Maxwell's equations (2) and (3)

$$curl\left(\rho curl\mathbf{T}\right) + \frac{\partial}{\partial t}\left[\mu\left(\mathbf{T} - grad\Phi\right)\right] = -\frac{\partial}{\partial t}\left(\mu\mathbf{T}_0\right), \tag{11}$$

$$div\left[\mu\left(\mathbf{T} - grad\Phi\right)\right] = -div\left(\mu\mathbf{T}_0\right) \tag{12}$$

remain to be solved in the **T**,Φ-Φ formulation.

Introducing the edge based vector basis functions $\mathbf{N}_i(\mathbf{r})$ (i = 1, 2, ..., n_e) and the node based scalar basis functions $N_i(\mathbf{r})$ (i = 1, 2, ..., n_n) in the finite elements (n_e is the number of edges and n_n the number of nodes in the finite element mesh, **r** denotes the space coordinates), the potentials are approximated as

$$\mathbf{A}(\mathbf{r},t) \approx \mathbf{A}_h(\mathbf{r},t) = \sum_{k=1}^{n_e} a_k(t)\mathbf{N}_k(\mathbf{r}),\ \mathbf{T}(\mathbf{r},t) \approx \mathbf{T}_h(\mathbf{r},t) = \sum_{k=1}^{n_e} t_k(t)\mathbf{N}_k(\mathbf{r}), \tag{13}$$

$$v(\mathbf{r},t) \approx v_h(\mathbf{r},t) = \sum_{k=1}^{n_n} v_k(t)N_k(\mathbf{r}),\ \Phi(\mathbf{r},t) \approx \Phi_h(\mathbf{r},t) = \sum_{k=1}^{n_n} \phi_k(t)N_k(\mathbf{r}). \tag{14}$$

The vector $\mathbf{T}_0$ is represented by edge basis functions similarly to **T** in (13). The coefficients for $\mathbf{T}_0$ are easily computed as its line integrals along the edges of the finite element mesh.

Applying Galerkin techniques to (9) and (10) leads to the following ordinary differential equations for the **A**,*v*-**A** formulation:

$$\int_{\Omega_c} curl\mathbf{N}_i \cdot \nu curl\mathbf{A}_h d\Omega + \frac{d}{dt}\int_{\Omega_c} \sigma\mathbf{N}_i \cdot \left(\mathbf{A}_h + gradv_h\right)d\Omega = \int_{\Omega_c} curl\mathbf{N}_i \cdot \mathbf{T_0} d\Omega, \qquad i=1,2,...,n_e, \tag{15}$$

$$\frac{d}{dt}\int_{\Omega_n+\Omega_c} \sigma gradN_i \cdot \left(\mathbf{A}_h + gradv_h\right)d\Omega = 0, \qquad i=1,2,...,n_n. \tag{16}$$

Gathering the unknown time functions $a_k(t)$ (k = 1, 2, ..., n_e) and $v_k(t)$ (i = 1, 2, ..., n_n) in (13) and (14) in a vector $\mathbf{x}(t)$, the matrix form of (15), (16) is the system of ordinary differential equations

$$\mathbf{S}\left[\nu\left(\mathbf{x}(t)\right)\right]\mathbf{x}(t) + \mathbf{M}(\sigma)\frac{d\mathbf{x}(t)}{dt} = \mathbf{f}(t) \tag{17}$$

where: the dependence of the stiffness matrix **S** on ν and of the mass matrix **M** on σ is explicitly shown. Since the reluctivity depends on the field, ν depends on **x** and hence on *t* as indicated. The right hand side vector is denoted by **f**.

In a similar manner, Galerkin's method applied to (11) and (12) results in the ordinary differential equations

$$\int_{\Omega_c} curl\mathbf{N}_i \cdot \rho curl\mathbf{T}_h d\Omega + \frac{d}{dt}\int_{\Omega_c} \mu\mathbf{N}_i \cdot \left(\mathbf{T}_h - grad\Phi_h\right) d\Omega = -\frac{d}{dt}\int_{\Omega_c} \mu\mathbf{N}_i \cdot \mathbf{T_0} d\Omega\,, \qquad i=1,2,...,n_e, \tag{18}$$

$$-\frac{d}{dt}\int_{\Omega_n+\Omega_c} \mu grad N_i \cdot \left(\mathbf{T}_h - grad\Phi_h\right) d\Omega = \frac{d}{dt}\int_{\Omega_n+\Omega_c} \mu grad N_i \cdot \mathbf{T_0} d\Omega\,, \qquad i=1,2,...,n_n \tag{19}$$

for the **T**,Φ-Φ formulation. The vector **x**(*t*) now consists of the unknown time-dependent coefficients $t_k(t)$ (k = 1, 2, ..., n_e) and $\phi_k(t)$ (k= 1, 2, ..., n_n) in (13) and (14). The matrix form of the Galerkin equations is the system of ordinary differential equations

$$\mathbf{S}(\rho)\mathbf{x}(t) + \frac{d}{dt}\left[\mathbf{M}\left(\mu\left(\mathbf{x}(t)\right)\right)\mathbf{x}(t)\right] = \frac{d}{dt}\mathbf{g}\left(\mu\left(\mathbf{x}(t)\right),t\right) \tag{20}$$

where: the stiffness matrix S is now independent of x and hence of time, but the mass matrix M depends on the permeability which is itself field- and time-dependent. The product of the mass matrix and the unknown vector is differentiated with respect to time. The excitation vector g depends on x and t, and its time-derivative appears on the right hand side.

1.2. Harmonic balance method

The right hand side vectors of the systems of ordinary differential equations (17) and (20) are time periodic, i.e. $\mathbf{f}(t) = \mathbf{f}(t+T)$ and $\mathbf{g}(\mu,t) = \mathbf{g}(\mu,t+T)$ where T = 1/f is the period determined by the frequency f of the excitation, i.e. of the winding currents of the transformer. Since we are only interested in the steady state periodic solution satisfying the periodicity condition $\mathbf{x}(t) = \mathbf{x}(t+T)$, the solution is approximated by a complex Fourier series with N harmonics as

$$\mathbf{x}(t) \approx \mathbf{x}_N(t) = \mathrm{Re}\left(\sum_{k=1}^{N} \mathbf{X}_k e^{jk\omega t}\right) \tag{21}$$

where: j is the imaginary unit, □=2□f is the angular frequency of the excitation and Xk is the complex Fourier coefficient of the k-th harmonic at the angular frequency k□. It can be computed as

$$\mathbf{X}_k = \mathcal{F}_k(\mathbf{x}) = \frac{1}{T}\int_0^T \mathbf{x}(t) e^{-jk\omega t} dt\,. \tag{22}$$

Setting the approximation (21) into (17) and (20), respectively, and computing the N Fourier coefficients of both sides, a system of equations with N times as many unknowns is obtained as there are unknown time-functions, i.e. degrees of freedom, in **x**(*t*):

$$\mathcal{F}_m\left\{\mathbf{S}\left[\nu\left(\mathbf{x}_N\right)\right]\mathbf{x}_N\right\} + jm\omega\mathbf{M}(\sigma)\mathbf{X}_m = \mathcal{F}_m\left(\mathbf{f}\right), \qquad m = 1, 2, ..., N, \tag{23}$$

$$\mathbf{S}(\rho)\mathbf{X}_m + \mathcal{F}_m\left\{\frac{d}{dt}\left[\mathbf{M}\left(\mu\left(\mathbf{x}_N\right)\right)\mathbf{x}_N\right]\right\} = \mathcal{F}_m\left[\frac{d}{dt}\mathbf{g}\left(\mu\left(\mathbf{x}_N\right),t\right)\right], \qquad m = 1, 2, ..., N. \tag{24}$$

In the linear terms in (23) and (24), the Fourier coefficients of the m-th harmonic appear only. The time derivative in (17) corresponds to a multiplication by $jm\omega$ in (23). The right hand side of (23) can be computed directly from **f** as shown in (22). On the other hand, the nonlinear terms containing the permeability $\mu(\mathbf{x}_N)$ or the reluctivity $\nu(\mathbf{x}_N)$ depending on the unknown solution (21) couple all Fourier coefficients to each other. Therefore, due to the nonlinearity, one cannot solve for each harmonic alone, a fact which significantly increases the complexity of the problem.

2. DECOUPLING OF HARMONICS

It is highly desirable that the harmonics be decoupled and hence be determined independent of each other. This would lead to *N* systems of equations, each with as many unknowns as there are degrees of freedom in the FEM approximation. As shown below, the decoupling is trivial in the linear case but, for nonlinear problems, special techniques are needed.

2.1. Linear problems

If the permeability and the reluctivity are independent of the magnetic field, the systems of ordinary differential equations (17) and (20) become linear, since **S** in (17) and **M** in (20) do not depend on **x**(*t*). Hence, the Fourier coefficients indicated by $\mathcal{F}_m$ in (23) and (24) become

$$\mathcal{F}_m\left\{\mathbf{S}(\nu)\mathbf{x}_N\right\} = \mathbf{S}(\nu)\mathbf{X}_m, \quad \mathcal{F}_m\left\{\frac{d}{dt}\left[\mathbf{M}(\mu)\mathbf{x}_N\right]\right\} = jm\omega\mathbf{M}(\mu)\mathbf{X}_m, \quad \mathcal{F}_m\left[\frac{d}{dt}\mathbf{g}(\mu,t)\right] = jm\omega\mathcal{F}_m(\mathbf{g}) \tag{25}$$

Hence, (23) and (24) indeed become decoupled, each harmonic can be determined independently:

$$\left[\mathbf{S}(\nu) + jm\omega\mathbf{M}(\sigma)\right]\mathbf{X}_m = \mathcal{F}_m(\mathbf{f}), \qquad \text{m = 1, 2, ..., N,} \tag{26}$$

$$\left[\mathbf{S}(\rho) + jm\omega\mathbf{M}(\mu)\right]\mathbf{X}_m = jm\omega\mathcal{F}_m(\mathbf{g}), \qquad \text{m = 1, 2, ..., N.} \tag{27}$$

The right hand side vectors in (26) and (27) can be easily computed by traditional Fourier decomposition as in (22).

2.2. Fixed point iteration technique for nonlinear problems

The fixed point iteration method for the solution of nonlinear equations reduces the problem to finding the fixed point of a nonlinear function. The fixed point $\mathbf{x}_{FP}$ of the function **G**(**x**) is defined as

$$\mathbf{x}_{FP} = \mathbf{G}(\mathbf{x}_{FP}). \tag{28}$$

The fixed point can be determined as the limit of the sequence

$$\mathbf{x}^{(s+1)} = \mathbf{G}\left(\mathbf{x}^{(s)}\right), \qquad \text{s = 0, 1, 2, ... ,} \tag{29}$$

provided **G**(**x**) is a contraction, i.e. there exists a contraction number $-1 < q < 1$ so that for any **x** and **y**

$$\left\|\mathbf{G}(\mathbf{x}) - \mathbf{G}(\mathbf{y})\right\| \le q\left\|\mathbf{x} - \mathbf{y}\right\| \tag{30}$$

where: $\|\cdot\|$ is a suitable norm. Furthermore, the sequence (29) converges to the same fixed point independent of the choice of the initial guess $\mathbf{x}^{(0)}$.

A general nonlinear equation **F**(**x**)=**0** can be transformed to a fixed point problem by selecting a suitable linear operator **A** and defining **G** as

$$\mathbf{G}(\mathbf{x}) = \mathbf{x} + \mathbf{A}^{-1}\mathbf{F}(\mathbf{x}). \tag{31}$$

The fixed point iterations (29) then become

$$\mathbf{A}^{(s)}\mathbf{x}^{(s+1)} = \mathbf{A}^{(s)}\mathbf{x}^{(s)} + \mathbf{F}\left(\mathbf{x}^{(s)}\right), \qquad \text{s = 0, 1, 2, ...} \tag{32}$$

where: the superscript *s* of $\mathbf{A}^{(s)}$ indicates that the linear operator **A** can be changed at each iteration step to accelerate convergence.

In case of the ordinary differential equations (17) and (20) obtained by Galerkin FEM techniques, the selection of a linear operator is straightforward: the permeability or reluctivity has to be set to a value independent of the magnetic field. This value, μ_{FP} or ν_{FP}, is not necessarily independent of the space coordinates **r**, i.e. generally $\mu_{FP} = \mu_{FP}(\mathbf{r})$ or $\nu_{FP} = \nu_{FP}(\mathbf{r})$ are permeability or reluctivity distributions varying in the problem domain but independent of the field and hence of time. By the same argument as

the one used for the linear operator **A** above, μ_{FP} or ν_{FP} can also change at each iteration step. This fixed point permeability or reluctivity function will be denoted by $\mu_{FP}^{(s)}$ or $\nu_{FP}^{(s)}$ below.

Once a suitable fixed point permeability or reluctivity has been selected, (17) and (20) can be iteratively solved by obtaining $\mathbf{x}^{(s+1)}(t)$ from the equations

$$\mathbf{S}\left(\nu_{FP}^{(s)}\right)\mathbf{x}^{(s+1)}(t)+\mathbf{M}(\sigma)\frac{d\mathbf{x}^{(s+1)}(t)}{dt}=\mathbf{S}\left(\nu_{FP}^{(s)}-\nu^{(s)}\right)\mathbf{x}^{(s)}(t)+\mathbf{f}(t)\quad s=\ 0,\ 1,\ 2,\ ... \tag{33}$$

$$\mathbf{S}(\rho)\mathbf{x}^{(s+1)}(t)+\frac{d}{dt}\left[\mathbf{M}\left(\mu_{FP}^{(s)}\right)\mathbf{x}^{(s+1)}(t)\right]=\frac{d}{dt}\left[\mathbf{M}\left(\mu_{FP}^{(s)}-\mu^{(s)}\right)\mathbf{x}^{(s)}(t)\right]+\frac{d}{dt}\mathbf{g}\left(\mu^{(s)},t\right)\quad s=\ 0,\ 1,\ 2,\ ... \tag{34}$$

at each step. The permeability or reluctivity distribution $\mu^{(s)}$ or $\nu^{(s)}$ are determined from the solution $\mathbf{x}^{(s)}(t)$ i.e., in contrast to $\mu_{FP}^{(s)}$ or $\nu_{FP}^{(s)}$, they are time dependent. The stiffness matrix **S** on the right hand side of (33) is obtained with ν replaced by $\nu_{FP}^{(s)}-\nu^{(s)}$ and the mass matrix **M** on the right hand side of (34) is computed with $\mu_{FP}^{(s)}-\mu^{(s)}$ written instead of μ. Indeed, these matrices depend linearly on ν and μ, respectively.

Since (33) and (34) are linear ordinary differential equation systems, they can be solved by the harmonic balance method with decoupled harmonics as in (26) and (27). The corresponding equations to be solved for *s* = 0, 1, 2, ... are:

$$\left[\mathbf{S}\left(\nu_{FP}^{(s)}\right)+jm\omega\mathbf{M}(\sigma)\right]\mathbf{X}_m^{(s+1)}=\mathcal{F}_m\left[\mathbf{S}\left(\nu_{FP}^{(s)}-\nu^{(s)}\right)\mathbf{x}^{(s)}(t)+\mathbf{f}(t)\right],\ldots.m=1,\ 2,\ ...,\ N, \tag{35}$$

$$\left[\mathbf{S}(\rho)+jm\omega\mathbf{M}\left(\mu_{FP}^{(s)}\right)\right]\mathbf{X}_m^{(s+1)}=jm\omega\mathcal{F}_m\left[\mathbf{M}\left(\mu_{FP}^{(s)}-\mu^{(s)}\right)\mathbf{x}^{(s)}(t)+\mathbf{g}\left(\mu^{(s)},t\right)\right],\ldots.m=1,\ 2,\ ...,\ N \tag{36}$$

where: $\mathbf{x}^{(s)}(t)$ is obtained from the harmonics similarly to (21) as

$$\mathbf{x}^{(s)}(t)=\mathrm{Re}\left(\sum_{k=1}^{N}\mathbf{X}_k^{(s)}e^{jk\omega t}\right). \tag{37}$$

The nonlinear iterations are terminated once the change of $\mu^{(s)}$ or $\nu^{(s)}$ between two iteration steps becomes less than a suitable threshold.

The most computational effort is needed for the solution of the *N* linear equation systems in (35) and (36), respectively. Since these are independent of each other, they can be solved parallel with each core responsible for the solution for one harmonic $\mathbf{X}_m^{(s+1)}$. Once these parallel computations are ready, the right hand side for the next iteration can be determined by first computing the time function of the solution as in (37) and then carrying out the Fourier decompositions indicated in (35) and (36). This is the part of the process when no parallelization is possible, but since the computational effort necessary for it is negligible in comparison to the solution of the large linear algebraic systems, the method is massively parallel.

One of the most important factors influencing the rate of the convergence of the fixed point technique is the choice of the fixed point permeability or reluctivity. As pointed out above, this is not necessarily constant with respect to the space coordinates, i.e. it can be selected to be different at each Gaussian integration point of the finite element mesh. The analysis of the optimal choice has been carried out in [4], the result for $\mu_{FP}^{(s)}$ below is taken from there:

$$\mu_{FP}^{(s)}=\max\left\{\frac{\int_0^T\left[\mu^{(s)}\right]^2dt}{\int_0^T\mu^{(s)}dt},\frac{\min\limits_{t\in[0,T]}\left(\mu^{(s)}\right)+\max\limits_{t\in[0,T]}\left(\mu^{(s)}\right)}{2}\right\}. \tag{38}$$

The optimal fixed point reluctivity is obtained in a similar way. The permeability $\mu^{(s)}$ and the reluctivity $\nu^{(s)}$ are functions of the space coordinates and also of time since they are determined by the magnetic field distribution, itself space and time-dependent. According to (38), the fixed point permeability depends on the space coordinates but not on time. The computational effort necessary for the evaluation of (38) in each nonlinear iteration step is negligible.

3. COMPUTATION OF TRANSFORMER LOSSES

The eddy current losses of a transformer can be obtained by integrating the Joule loss density computed from the current density distribution. The current density can be computed from the potentials as shown in (6) and (7) in case of the **A**,*v*-**A** formulation and as given in (8) for the **T**,Φ-Φ formulation. Since the potentials are provided as Fourier series of the form (21) by the harmonic balance method presented, the current density is obtained as

$$\mathbf{J}(\mathbf{r},t) \approx \mathrm{Re}\left(\sum_{k=1}^{N} \mathbf{J}_k(\mathbf{r}) e^{jk\omega t} \right) \tag{39}$$

where: $\mathbf{J}_k(\mathbf{r})$ is the complex amplitude of the *k*-th harmonic of the current density. Hence, the eddy current losses are obtained as

$$P_{eddy} = \frac{1}{T}\int_0^T \left(\int_{\Omega_c} \frac{|\mathbf{J}(\mathbf{r},t)|^2}{\sigma} d\Omega \right) dt = \frac{1}{2}\sum_{k=1}^{N} \int_{\Omega_c} \frac{|\mathbf{J}_k(\mathbf{r})|^2}{\sigma} d\Omega \,. \tag{40}$$

The iron losses can be computed by integrating the specific losses per unit volume given as a function $p(|\mathbf{B}|)$ of the flux density provided by the manufacturer as described in [1] for the case of sinusoidal time variation. In fact, the specific losses are customarily given for unit weight but multiplying them by the specific weight yields the losses per unit volume. Usually, the specific losses are measured for one single frequency f_0 (e.g. f_0=50 Hz), this is denoted by $p(|\mathbf{B}|, f_0)$. In order to approximately take account of the dependence of the specific losses on frequency, the following algorithm is adopted. It is assumed that

$$p(|\mathbf{B}|, f) = p_{cl}(|\mathbf{B}|) f^2 + p_{hyst}(|\mathbf{B}|) f \tag{41}$$

where: $p_{cl}(|\mathbf{B}|) = \frac{\sigma \pi^2 d^2}{6} |\mathbf{B}|^2$, (*d* is the thickness of the laminates, see [8]). Hence, $p_{hyst}(|\mathbf{B}|)$ can be obtained as

$$p_{hyst}(|\mathbf{B}|) = \frac{1}{f_0}\left[p(|\mathbf{B}|, f_0) - \frac{\sigma \pi^2 d^2}{6} |\mathbf{B}|^2 f_0^2 \right], \tag{42}$$

and, finally,

$$p(|\mathbf{B}|, f) = \frac{\sigma \pi^2 d^2}{6} |\mathbf{B}|^2 f^2 + \frac{f}{f_0}\left[p(|\mathbf{B}|, f_0) - \frac{\sigma \pi^2 d^2}{6} |\mathbf{B}|^2 f_0^2 \right]. \tag{43}$$

Similarly to the current density, the magnetic flux density is also obtained in the form of a Fourier series when using the harmonic balance technique:

$$\mathbf{B}(\mathbf{r},t) \approx \mathrm{Re}\left(\sum_{k=1}^{N} \mathbf{B}_k(\mathbf{r}) e^{jk\omega t} \right). \tag{44}$$

In lack of any better assumption, the specific losses are simply computed for each harmonic from (43) and then added:

$$P_{iron} = \sum_{k=1}^{N} \int_{\Omega} p\left(|\mathbf{B}_k|, k\omega/2\pi\right) d\Omega \,. \tag{45}$$

As an example, the autotransformer analyzed in [1] is presented here. Its name plate data are given in Table I.

Table I- Name Plate Data of a Single-phase Autotransformer

Rated Power	450/450/85 MVA
System Voltage	500/√3//230√3//13.8 kV
Rated Current	1559/3389/6159 A

The FEM model used has been improved in comparison to [1], it consists of 334,110 finite elements. The problem has been solved using the **T**,Φ-Φ formulation, resulting in 2,217,625 degrees of freedom for the potentials. The model is shown in Fig. 1.

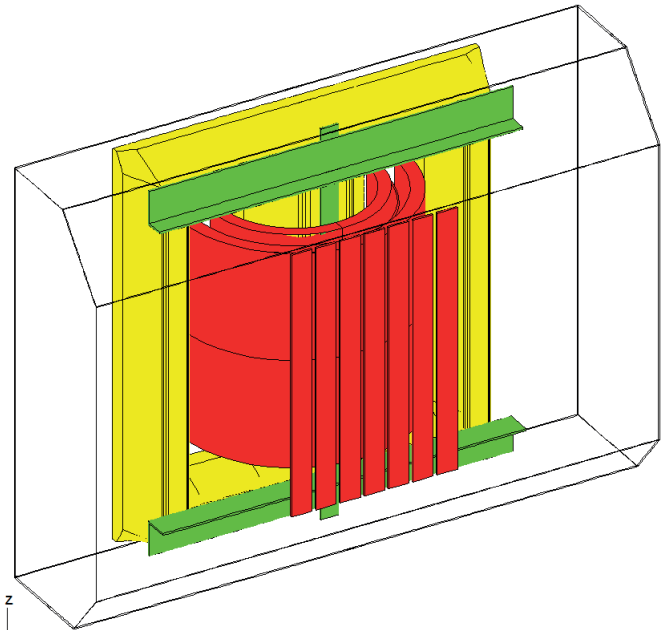

Figure 1 - FEM model of the analyzed single-phase autotransformer. The model comprises one half of the transformer. The tank is shown transparent, the core is yellow, the clamping plates and the tie bars are shown green. The windings and the tank shieldings are red.

Two short circuit computations have been carried out with the winding currents taken to be sinusoidal and the magnetization current neglected. In one of them, the method of [1] assuming sinusoidal time variation for all field quantities has been used and, in the second one, the harmonic balance method of the present paper using *N*=9 harmonics has been employed (only odd harmonics appear in the field quantities). The losses have been computed as described above. The computed losses in the two cases are summarized in Tables II and III, given as a percentage of the total measured short circuit losses.

Table II - Losses in Percentage of Total Measured Losses of Autotransformer Analyzed. All Quantities are Sinusoidal

DC copper losses (measured)	66.92%
AC copper losses (computed from 2D FEM)	21.75%
Tank (computed from model presented)	3.76%
Clamping plates (computed from model presented)	2.80%
Tie bars (computed from model presented)	0.21%
Tank shielding (computed from model presented)	0.51%
Core (computed from model presented)	2.75%
Total	98.70%

Table III- Losses in Percentage of Total Measured Losses of Autotransformer Analyzed. Harmonics up to the 9th are taken into Account

DC copper losses (measured)	66.92%
AC copper losses (computed from 2D FEM)	21.75%
Tank (computed from model presented)	2.55%
Clamping plates (computed from model presented)	2.08%
Tie bars (computed from model presented)	0.18%
Tank shielding (computed from model presented)	0.97%
Core (computed from model presented)	6.05%
Total	100.50%

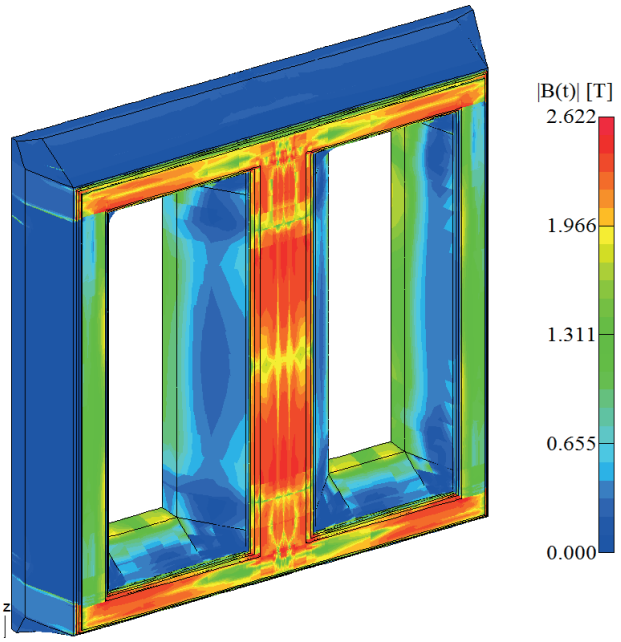

Figure 2 – Magnetic flux density in the core at the time instant of maximal winding current

These results indicate that in parts of the transformer where significant saturation is present, like in the first laminates of the core exposed to stray magnetic fields (see Figure 2), the losses due to the higher harmonics are considerable.

4. CONCLUSION

It has been shown that the use of FEM in conjunction with the harmonic balance method is capable of providing the solution to large, complex real-world problems with higher harmonics due to nonlinearity allowed for, and can hence be incorporated in the design cycle of large transformers. Taking account of the additional losses due to the higher harmonics in strongly saturated parts of the transformer improves the agreement of the computed losses with measurements.

REFERENCES

[1] O. Bíró, U. Baumgartner, K. Preis, G. Leber, “Numerical modeling of transformer losses”, Proceedings of the International Colloquium Transformer Research and Asset Management, Cavtat, Croatia, November 12 – 14, 2009, Session I, Numerical Modeling, 9 pages

[2] R. Albanese et al., “Periodic solutions of nonlinear eddy current problems in three-dimensional geometries”, IEEE Transactions on Magnetics, 28 (1992), 1118-1121

[3] O. Bíró and K. Preis, “An efficient time domain method for nonlinear periodic eddy current problems”, IEEE Transactions on Magnetics, 42, (2006), 695–698.

[4] G. Koczka et al., “Optimal convergence of the fixed-point method for nonlinear eddy current problems”, IEEE Transactions on Magnetics, 45 (2009), 948-951.

[5] G. Koczka et al., “Optimal fixed-point method for solving 3D nonlinear periodic eddy current problems”, COMPEL, 28 (2009), 1059-1067.

[6] G. Koczka and O. Bíró, “Fixed-point method for solving nonlinear periodic eddy current problems with T,Φ-Φ formulation”, COMPEL, 29 (2010), 1444-1452.

[7] O. Bíró et al., “Fast time-domain finite element analysis of 3D nonlinear time-periodic eddy current problems with T,Φ-Φ formulation”, IEEE Transactions on Magnetics, 47 (2011), 1170-1173.

[8] G. Bertotti, “Hysteresis in Magnetism”. Academic Press, 1998.